JOURNAL OF ENERGY TECHNOLOGY
Vol. 18, No. 4, pp. 189–202, December 2025

APPROXIMATE, NUMERICAL AND EXPERIMENTAL INVESTIGATIONS OF A WATER HAMMER IN VRHOVO BULB-TURBINE HYDROELECTRIC POWER PLANT

Original Scientific Article

Submitted
24. 11. 2025

Accepted
2. 12. 2025

Published
31. 12. 2025

ANTON BERGANT,[1, 2] JOŠT PEKOLJ[1]

[1] Litostroj Power d.o.o., Ljubljana, Slovenia
anton.bergant@litostrojpower.eu, jost.pekolj@litostrojpower.eu
[2] University of Ljubljana, Faculty of Mechanical Engineering, Ljubljana, Slovenia
anton.bergant@fs.uni-lj.si

CORRESPONDING AUTHOR
anton.bergant@litostrojpower.eu

Abstract This paper investigates the effectiveness and accuracy of approximate and numerical water hammer models in the Slovenian lower Sava River hydroelectric power plants with bulb turbines. An approximate model is introduced first, followed by numerical rigid water hammer models. Comparisons of the computed and measured results are examined for the transient load case of an emergency shutdown in Vrhovo hydroelectric power plant. The water hammer is mitigated by adjusting the guide vane and runner blade closing/opening laws properly. The results show a good agreement between the approximate and numerical and measured results.

Keywords
hydroelectric power plant,
bulb turbine,
water hammer,
computation,
field test, comparison study

https://doi.org/10.18690/jet.18.4.189-202.2025

1 Introduction

Hydroelectric power plants are flexible in both operation and energy storage (large water reservoirs) [1]. Both aspects are important for the stability of the electric power grid, due to the increasing share of variable renewable energy sources. This paper focuses on water hammer events in bulb turbine hydroelectric power plants located on the lower Sava River in Slovenia. The river flows through the Sava River basin, which is the largest basin in Slovenia and represents more than 50% of the national territory, but is the least utilised in terms of hydropower, with a total installed capacity of 230 MW [2]. The hydroelectric power plants (HEPPs) with bulb turbines on the lower Sava River are (from north to south): Vrhovo HEPP (1993, 3×11 MW) and Boštanj HEPP (2006, 3×10.9 MW). The completion of the hydropower cascade on the lower Sava River is under way (including the planned Mavčiče HEPP with three bulb turbines).

Variations in the discharge of a hydraulic turbine induce higher dynamic loads on the plant components, because of the water hammer phenomena [3, 4]. The consequences of water hammer can result in damage to the turbine and hydromechanical equipment (turbine blade failure), to elements of the flow-passage system (pipe rupture), or in operational disturbances (plant outage). For utility owners, this translates into increased costs associated with repairs, repeated maintenance activities and a decrease in electricity generation. Therefore, excessive water hammer-induced loads in hydroelectric power plants must be limited to the values prescribed by the relevant research and Standards [5, 6].

Water hammer in hydroelectric power plants with bulb turbines can be controlled within the prescribed limits through a combination of several methods [3, 6, 7]. One of the most effective methods is the modification of the operational regimes. This involves finding the most suitable combination of the guide vane and runner blade closing and opening laws. A two-speed or multi-speed guide vane servomotor closing ramp (with an added cushioning time) can, in many cases, improve the operational safety of the plant significantly. The next method is to install surge control devices in the system. For example, a draft tube gate can prevent the occurrence of runaway conditions in a bulb turbine. Similarly, the sluicing operation of the bulb turbines and installation of a by-pass valve can attenuate open channel waves during transient events. In essence, these devices modify the dynamic

response of the plant component characteristics (for example, by increasing the effective inertia of the turbine unit rotating parts). Another method of water hammer protection is the redesign of the flow passage layout. The redesign may include changes to the conduit geometry, such as diameter and length, or repositioning of key system components (e.g., gates). Finally, the water hammer safety measure can be the limitation of the plant's operating range. This can be done by imposing restrictions on the discharge, gross head, or unit power, to reduce the magnitude of extreme water hammer loads.

The most common water hammer control device in bulb turbine hydroelectric power schemes is the turbine governor coupled to the guide vane and runner blade servomotor mechanisms [8, 9]. The control devices should operate smoothly in the following normal operating conditions [6]: turbine start-up, load acceptance, load reduction, load rejection under governor control and emergency shutdown. Emergency conditions occur when one of the safety elements fails, which can cause partial turbine runaway. The full-turbine runaway is considered as a catastrophic transient regime. It occurs when several safety elements fail in the most unfavourable way. Water hammer analysis should be performed for normal, emergency and catastrophic operating conditions [6].

The main aim of this study is to validate three different computational water hammer models, including an approximate model [10], and one-dimensional (1D) [11] and three-dimensional (3D) [12], [13] numerical rigid water hammer models. The results obtained from these simulations are then compared with the measurement data collected at the Vrhovo HEPP. Comparisons of the computed and measured results are examined for a normal operating transient regime.

2 Theoretical modelling

Hydraulic transients in hydroelectric power plants equipped with bulb turbines can be analysed using either the elastic [3, 7] or rigid [7, 11] water hammer theories. Run-of-river power plants comprise relatively short inlet and outlet conduits, where the conduit length is of the same order of magnitude as the cross-sectional dimensions. This is also the case for the Vrhovo HEPP examined in this paper. The cross-sectional area often has a complex shape. Under these conditions, standard one-dimensional elastic water hammer models may not capture the wave transmission

and reflection phenomena accurately. For such cases, the rigid water hammer model is generally recommended [11], assuming an incompressible liquid and rigid pipe walls. Using this rigid model theory, the dynamics of unsteady pipe flow are described by the one-dimensional equation of motion [3]:

$$\frac{1}{\rho g}\frac{\partial p}{\partial x}+\frac{fQ|Q|}{2gDA^2}+\frac{1}{gA}\frac{dQ}{dt}=0 \tag{1}$$

in which p = pressure, ρ = liquid density, g = gravitational acceleration, f = the Darcy-Weisbach friction factor, x = distance, Q = discharge, D = conduit diameter, t = time, and A = cross-sectional area. The symbols are defined as they first appear in the paper. Equation (1) is solved together with the dynamic equation of the unit rotating masses considering the turbine performance characteristics [11]:

$$T_x = I\frac{d\omega}{dt} \tag{2}$$

in which T_x = the turbine net torque, ω = angular velocity, and I = the polar moment of inertia. The one-dimensional equation of motion for an unsteady conduit flow (Eq. (1)) can be solved either separately or simultaneously with the dynamic torque equation (Eq. (2)). Đorđević [10] developed approximate solutions of Eqs. (1) and (2) applied to the turbine emergency shutdown case separately as follows:

(i) The maximum transient pressure due to the linear single-stage closure of the turbine:

$$p_{max}=\left(1+\frac{2\sigma}{2-\sigma}\right)p_0+\rho g\Delta z+\Delta p_{loss} \tag{3}$$

in which σ = the water hammer coefficient, Δz = the elevation difference between the tailwater and datum level, Δp_{loss} = the conduit pressure losses. The water hammer coefficient is calculated by the following equation:

$$\sigma=\frac{\rho g}{p_0}\cdot G=\frac{\rho g}{p_0}\cdot\sum\frac{L_i}{A_i} \tag{4}$$

in which G = a geometric characteristic and L = the length of the conduit.

(ii) The maximum transient rotational speed after the turbine shutdown:

$$n_{max} = n_0 \cdot \sqrt{1 + \frac{364 \cdot P_0 \cdot T_f' \cdot f_d}{mD^2 \cdot {n_0}^2}} \tag{5}$$

in which P_0 = the initial power [kW], $T_f' = 0.65 \cdot T_f$ = the modified linear closure time T_f [s], $f_d = 1+1.25 \cdot \sigma$ = the fluid dynamic coefficient, mD^2 = the total inertia of the turbine unit`s rotating parts [tm^2], n_0 = the initial speed of rotation [min^{-1}]. Equations (3) and (4) determine the maximum pressure and turbine rotational speed in a simple waterway, respectively. However, in most engineering studies we are interested in analysing the complete dynamic evolution of pressure and rotational speed variations throughout the water hammer event. This is important, because the superposition of pressure waves in complex systems can have a significant impact on the safety of the entire hydroelectric power system. Therefore, water hammer phenomena in hydroelectric power plants should be calculated using the time-dependent method [4].

Krivchenko et al. [11] developed a numerical method for simultaneous solution of Eqs. (1) and (2). The two equations are solved simultaneously with the aid of a fourth order Runge-Kutta numerical method. The numerical algorithm can be coded in one of the computer languages or mathematical simulation packages (Fortran code in our case). Time-dependent turbine behaviour is represented using laboratory-measured turbine characteristics. Naturally, some differences exist between the steady-state and unsteady performance curves, due primarily to unsteady flow effects in the turbine flow-passage domain and when cavitation occurs.

One-dimensional water hammer models are limited in their ability to capture certain high-frequency effects in conduits or hydraulic turbines, such as draft tube vortices and rotor–stator interactions [14]. Although the 1D model is used traditionally for water hammer analysis in HEPPs, its accuracy can be improved by incorporating terms that account for multidimensional effects [15]. In contrast, three-dimensional models enable the prediction of flow variables at any location within the computational domain. However, 3D unsteady flow models are computationally demanding, and defining the right boundary conditions in hydropower structures can be challenging. While certain approximations in 3D water hammer modelling [16] may have a negligible impact in some cases, they can lead to significant

systematic errors in others. Bergant and Kolšek presented a novel 3D model that is based on rigid water hammer principles tailored to bulb turbine hydropower schemes [12], [13].

The 3D model is based on the solution of the Reynolds averaged Navier-Stokes (RANS) equations coupled with the dynamic equation of the turbine unit rotating masses – Eq. (2). This method does not require a set of turbine performance characteristics data as in the 1D model. An incompressible liquid and rigid pipe walls are assumed in the model. The incompressible turbulent flow is described by the continuity equation and the Navier-Stokes equation. The Reynolds averaging yields the following two equations [17]:

$$\frac{\partial}{\partial t}\int_V \rho dV + \int_S \rho(\mathbf{v}-\mathbf{v}_s)\mathbf{n}dS = 0 \tag{6}$$

$$\frac{\partial}{\partial t}\int_V \rho\mathbf{v}dV + \int_S \rho\mathbf{v}(\mathbf{v}-\mathbf{v}_s)\mathbf{n}dS = \int_S(\boldsymbol{\tau}-\rho\overline{\mathbf{v}'\mathbf{v}'})\mathbf{n}dS + \int_V \mathbf{f}_b dV \tag{7}$$

in which V = volume, $\mathbf{v}$ = the flow velocity vector, $\mathbf{v}_s$ = the surface velocity vector, $\mathbf{n}$ = the unit vector, S = the surface, $\boldsymbol{\tau}$ = the stress tensor, $\rho\overline{\boldsymbol{v}'\boldsymbol{v}'}$ = the Reynolds stresses, and $\mathbf{f}_b$ = the vector of a body force per unit volume. The Reynolds stresses are calculated by the standard k-ε turbulence model [17]. Because the turbine CFD calculations involve a moving grid, the equation of space conservation must be satisfied as well:

$$\frac{\partial}{\partial t}\int_V dV + \int_S \rho\mathbf{v}_s\mathbf{n}dS = 0 \tag{8}$$

A computational domain is comprised of the whole turbine flow-passage system. A numerical finite volume method (FVM) is employed to approximate the RANS partial differential equations with algebraic ones. Bergant and Kolšek`s simulations [12], [13] used the CFD solver code ICCM COMET [18]. Their results will be used in this paper for comparison analysis.

3 Comparison between the computed and experimental results for a turbine shutdown case in the Vrhovo HEPP

Field test measurements are essential to validate an approximate model, and numerical 1D and 3D time dependent simulations. Validation of the approximate and numerical 1D water hammer models is performed traditionally by practising engineers, whereas 3D models remain the focus of active research in both industry and academia. In this study the computational results are validated against the measured results obtained in Vrhovo HEPP, Slovenia. The differences between the computed and measured results are examined for the case of an emergency shutdown of the turbine unit [12], [13].

3.1 Description of the Vrhovo HEPP

Vrhovo HEPP is the first power plant that was built in a planned chain of six run-off river type power plants on the Sava River in the south-east part of Slovenia in 1993. Vrhovo HEPP is comprised of the powerhouse and spillway structure. A vertical-slot entrance to the spawning area has been built on the right-hand-side riverbank (from the perspective of the flow direction) [19].

There are three bulb turbine units in Vrhovo HEPP, each of rated power P_r = 11.0 MW at the gross head H_g = 7.5 m. The turbine steady-state rotational speed is n_0 = 107.14 min^{-1} and the polar moment of inertia of the turbine unit rotating parts, including the added water mass [11], is mD^2 = 954.6 × 10^3 kgm^2. The turbine flow-passage system of the Vrhovo HEPP is comprised of an upper basin, a turbine inlet conduit, a horizontal-axis double-regulated bulb turbine, an outlet conduit and a tailrace - see Fig. 1. The dimensions of the inlet and outlet conduits used in the approximate method, and the one-dimensional rigid water hammer model, are expressed as the geometrical characteristics G_u = 0.288 m^{-1} and G_d = 0.557 m^{-1}, respectively (G_u only in the approximate model). The three-dimensional water hammer model considers dimensions in the actual 3D space. Water hammer in the power plant is controlled by adjusting the guide vane and runner blade closing/opening laws properly.

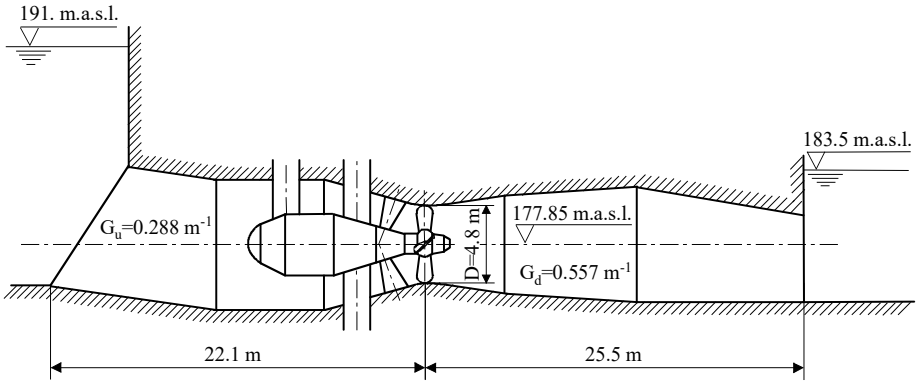

Figure 1: Layout of the Vrhovo HEPP bulb turbine flow-passage system
Source: own – adapted from [12, 13].

Field tests were performed to assess the adequacy of the designed guide vane and runner blade opening and closing laws for several water hammer scenarios, including the emergency shutdown of the turbine unit. During normal transient operating regimes, the focus lies on the two most important guaranteed parameters: (i) the maximum pressure at the turbine inlet together with the minimum pressure at the turbine outlet, and (ii) the maximum increase in the turbine unit rotational speed. These criteria were originally specified in IEC 60545:1976 [20] and most recently by IEC TS 63111:2025 [6]. Due to safety precautions, IEC 62006:2010 [21] recommends that the emergency shutdown tests should be carried out first during the commissioning of the turbine units. The results of field tests in Vrhovo HEPP showed that, for all normal operating transient regimes, the measured extreme values remained within the prescribed limits.

Continuous measurements of the guide vane and runner blade servomotor strokes y_{gv} and y_{rb}, respectively ($U_x = \pm 0.3$ %), the turbine unit rotational speed n ($U_x = \pm 0.1$ %), the pressure at the draft tube inlet p_{dt} ($U_x = \pm 0.3$ %), and the upper and lower basin water levels z_u and z_d, respectively ($U_x = \pm 0.3$ %) were carried out during an emergency shutdown of the turbine unit - see Fig. 2. The pressure in the vaneless space between the guide vanes and the runner blades, and the axial hydraulic force were measured as well, but are not considered in this paper – for details please see [12], [13]. The pressure at the turbine inlet conduit p_{ti} could not be measured due to

unavailable access during the test. The uncertainty in the measurement U_x is expressed as a root-sum-square combination of the bias and precision errors [22].

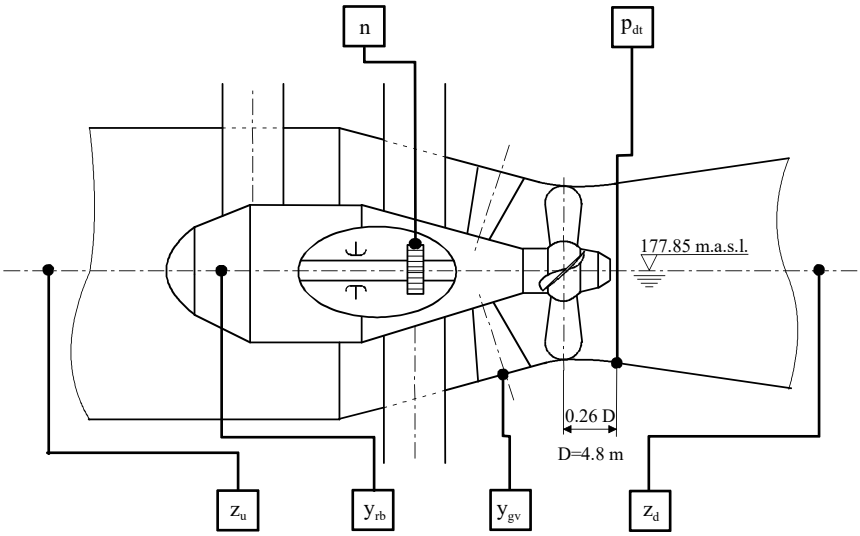

Figure 2: Position of the considered sensors for continuously measured quantities
Source: own – adapted from [12, 13].

3.2 Emergency shutdown of the bulb turbine in Vrhovo HEPP

The results are presented of an emergency shutdown of the turbine unit from the load of 10.2 MW. Initially, the electromagnetic torque of the generator drops to zero instantaneously. The guide vanes close gradually to their fully closed position, whereas the runner blades open to their fully open position. This is the most severe normal operating regime with respect to extreme transient loads at on-cam initial flow conditions.

Figure 3 shows the measured guide vane and the runner blade servomotor strokes for the considered case. A two-stroke guide vane servomotor stroke closing time function (adding a cushioning stroke) (Fig. 3a) and linear runner blade servomotor opening time function (Fig. 3b), improve the safe operation of the plant significantly (lower the maximum rotational speed rise and attenuate the pressure induced forces on the runner). The actual measured servomotor stroke was used as the input data

for the numerical 1D and 3D simulations. A linear closure time T_f = 6.0 s was considered for the approximate calculations.

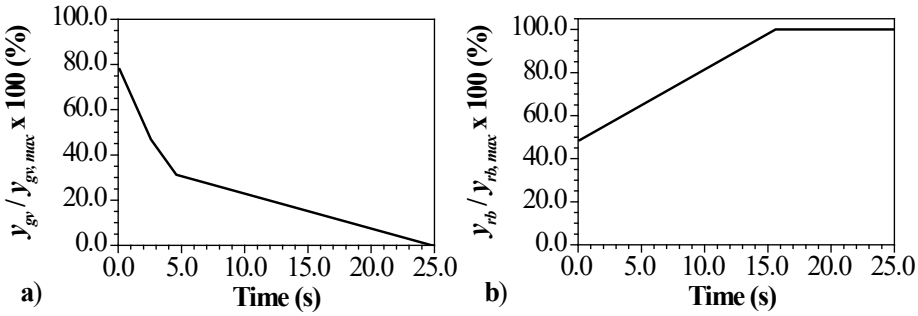

Figure 3: Guide vane (y_{gv}) and runner blade (y_{rb}) servomotor strokes
Source: own – adapted from [12, 13].

Figure 4 presents the variation of the turbine rotational speed during shutdown of the unit, which is an important regulation parameter. The agreement between the computed 1D- and 3D-model results, and the measured maximum speed rises of 48.9% and 49.4%, and 45.9%, respectively is reasonable (n_0 = 107.14 min^{-1}). The speed rise of 54.4% obtained by the approximate Eq. (5) is slightly higher than the two simulated values. Equation (5) does not consider the effect of the runner blade opening, which attenuates the maximum rotational speed rise. The computational and measured results are well within the originally proposed allowable speed rise of 75%.

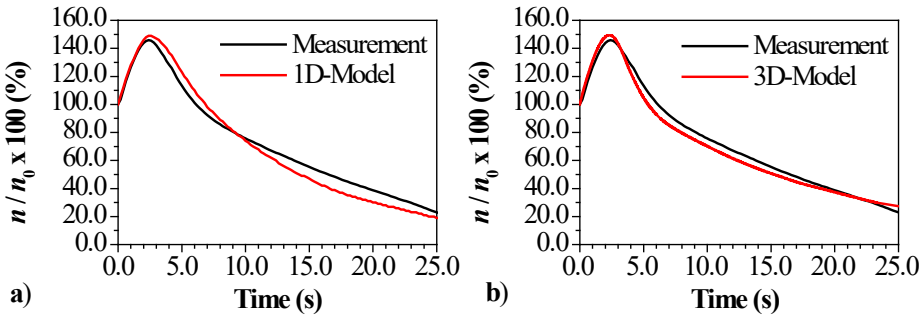

Figure 4: Computed and measured turbine rotational speed (n_0 = 107.14 min^{-1})
Source: own – adapted from [12, 13].

As stated in Section 3.1, pressure at the turbine inlet could not be measured due to unavailable access during the considered test. However, the pressure rise at the turbine inlet is an important design parameter in hydroelectric power plants with long penstocks (large water mass inertia). Figure 5 presents the turbine inlet pressure history for the 1D and 3D numerical simulations. In the case of the unit shutdown there is a maximum pressure rise of 5 % and 4 % predicted by the 1D- and 3D-models, respectively. The pressure rise predicted by Eq. (3) was 5.4%. The results calculated by the three methods are in close agreement. Finally, the maximum pressures at the datum level z = 177.85 m.a.s.l. obtained by the approximate, 1D and 3D numerical methods of 137 kPa, 136.5 kPa and 135.2 kPa, respectively, are less than the maximum allowable pressure of 169. kPa.

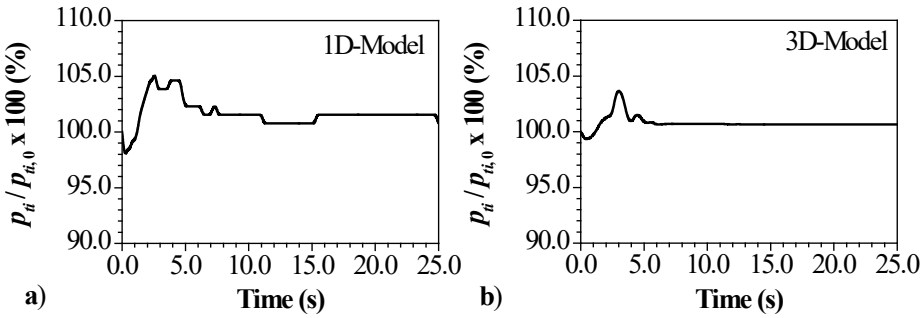

Figure 5: Computed turbine inlet conduit pressure ($p_{ti,0}$ = 130 kPa, datum level z = 177.85 m.a.s.l.)

Source: own – adapted from [12, 13].

Figure 6 compares the 1D and 3D numerically predicted and measured pressures in the draft tube inlet of the turbine (see Fig. 2). The draft tube pressure was measured at a distance of 1.25 m downstream from the runner vertical axis. The measured draft tube pressure exhibits water hammer low frequency pressure superimposed by high frequency pressure peaks that can be attributed to complex local flow behaviour in the draft tube inlet during the closure period. The minimum measured peak pressure of -25 kPa is well above the liquid vapour pressure of -100 kPa. The 1D-model predicted an average pressure at the draft tube inlet cross-sectional area at 2.02 m downstream from the runner vertical axis. The agreement of the average pressures is reasonable (Fig. 6a). However, the 1D numerical model was unable to

reproduce the multidimensional and multiphase flow phenomena occurring at the draft tube inlet accurately. The 3D-model captured single-phase unsteady flow effects in the runner space, and the agreement between the computed pressure and the measured pressure was better (Fig. 6b). These two pressures are compared at the same position. The discrepancies between the 3D and measured results are due to cavitational effects. This topic is a subject of the authors' further research. However, the minimum measured and computed pressures are well above the liquid vapour pressure head of -100 kPa (no danger of water column separation). Finally, there is no reliable approximate formula for the computation of the minimum draft tube pressure due to the complex flow field at the draft tube inlet, as discussed in our case study.

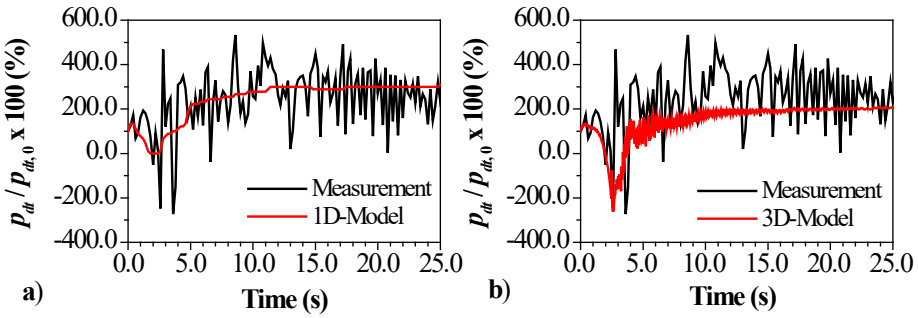

Figure 6: Computed and measured draft tube pressure ($p_{dt,0}$ = 9 kPa, datum level z = 177.85 m.a.s.l.)

Source: own – adapted from [12, 13].

4 Conclusions

The paper analyses methods for calculating hydraulic transients in hydroelectric power plants and measures for mitigation of transients. It introduces and describes the operation of the Vrhovo HEPP, which is part of the chain of hydropower plants on the lower Sava River in Slovenia. The main objective was to validate three different calculation methods for predicting transient parameters during an emergency shutdown of the bulb turbine against the site measured results. The first conclusion from the comparison of calculation and measurement results is that the extreme values of the critical transient parameters for the selected load case

(emergency shutdown from 92% load) are acceptable. The maximum rotational speed rise is always below the allowed rise of 75%, the maximum turbine inlet pressure rise is always below 6%, and the minimum draft tube pressure is always well above −100 kPa. This confirms that the selected two-stroke linear closing law of the guide vane and the linear opening law of the runner blade servomotors are acceptable for the presented load case.

The calculated maximum turbine inlet pressure rise obtained using the approximate, and 1D and 3D numerical rigid water hammer models agreed well, and are 5.4%, 5% and 4%, respectively.

The calculated maximum speed rise predicted by the 1D and 3D numerical models is 48.9% and 49.4%, respectively. These results are in close agreement, whereas the approximate method (Eq. 5) predicted a higher value of 54.4%. The difference is due mainly to the influence of the runner blade opening, which attenuates the rise in rotational speed. The measured peak speed rise was 45,9%, which is slightly lower than the values predicted by the calculation methods.

Larger discrepancies were observed in the calculated values of the draft tube inlet pressure. The 1D numerical model cannot represent the multidimensional multiphase flow effects at the draft tube inlet adequately, whereas the 3D method captured single-phase unsteady flow effects downstream from the runner and predicted considerably lower minimum pressure during the emergency shutdown, which matches the measured value better. The results from the approximate method are not available, as no reliable approximate formula exists for computing the minimum draft tube pressure because of the complex flow field at the draft tube inlet, as demonstrated in this case study.

Acknowledgment

The first author acknowledges the support of the Slovenian Research and Innovation Agency (ARIS) conducted through the programme P2-0162 gratefully.

References

[1] E. Vagnoni, D. Gezer, I. Anagnostopoulos, G. Cavazzini, E. Doujak, M. Hočevar, P. Rudolf: *The new role of sustainable hydropower in flexible energy systems and its technical evolution through innovation*, Renewable Energy, Vol. 230, Paper 120832, 2024

[2] A. Bergant, J. Mazij, J. Pekolj: *Theoretical and experimental investigations of a water hammer in Sava River Kaplan turbine hydropower plants,* Journal of Energy Technology, Vol. 17, Iss. 4, p.p. 11 - 20, 2024
[3] M.H. Chaudhry: *Applied Hydraulic Transients*, Springer, 2014
[4] A. Bergant, J. Mazij, J. Pekolj, K. Urbanowicz: *Issues related to water hammer in Francis-turbine hydropower schemes: A review*, Energies, Vol. 18, Paper 6404, 2025
[5] S. Pejović, A.P. Boldy, D. Obradović: *Guidelines to Hydraulic Transient Analysis*, Gower Technical Press Ltd., 1987
[6] IEC TS 63111: *Hydraulic Turbines, Storage Pumps and Pump-Turbines – Hydraulic Transient Analysis, Design Considerations and Testing*, International Electrotechnical Commission, 2025
[7] E. B. Wylie, V. L. Streeter: *Fluid Transients in Systems*, Prentice Hall, 1993
[8] J. Fašalek, S. Rakčević: *Air valves and control of the Kaplan turbine during transients,* 13th IAHR Symposium on Hydraulic Machinery and Cavitation, Montréal, 1986
[9] J.H. Gummer: *Predicting draft tube water column separation in Kaplan turbine,* The International Journal of Hydropower & Dams, Vol. 10, Iss. 3, p.p. 80 - 83, 2003
[10] B. Đorđević: *Korišćenje Vodnih Snaga. Objekti Hidroelektrana (Use of Water Power. Hydraulic Power Plant Facilities),* Građevinski fakultet and Naučna knjiga, 1984 (in Serbian)
[11] G.I. Krivčenko, N.N. Aršenevski, E.V. Kvjatovskaja, V.M. Klabukov: *Gidromehaničeskie Perehodnie Processi v Gidroenergetičeskih Ustanovkah (Hydromechanical Transient Regimes in Hydroelectric Power Plants)*, Energija, 1975 (in Russian)
[12] A. Bergant, T. Kolšek: *Developments in bulb turbine three-dimensional water hammer modelling,* 21st IAHR Symposium on Hydraulic Machinery and Cavitation, Lausanne, 2002
[13] A. Bergant, T. Kolšek: *Comparison of one- and three-dimensional models for water hammer analysis in bulb turbine hydropower plants,* 9th International Conference on Pressure Surges, Chester, 2004
[14] S. Salehi, H. Nilsson, E. Lillberg, N. Edh: *An in-depth numerical analysis of transient flow field in a Francis turbine during shutdown,* Renewable Energy, Vol. 179, p.p. 2322 - 2347, 2021
[15] A. Bergant, Z. Rek, K. Urbanowicz: *Numerical 1D and 3D water hammer investigations in a simple pipeline apparatus,* Strojniški vestnik – Journal of Mechanical Engineering, Vol. 71, Iss. 5-6, p.p. 149 - 156, 2025
[16] C. Trivedi, O.G. Dahlhaug: *A comprehensive review of verification and validation techniques applied to hydraulic turbines,* International Journal of Fluid Machinery and Systems, Vol. 12, Iss. 4, p.p. 345 - 367, 2019
[17] J.H. Ferziger, M. Perić: *Computational Methods for Fluid Dynamics*, Springer-Verlag, 1999
[18] ICCM GmbH: *Comet Version 2.00. User Manual*, Institute of Computational Mechanics, 2000
[19] G. Kolman, M. Mikoš, M. Povž: *Ribji prehodi na hidroenergetskih pregradah v Sloveniji (Fish passages on hydroelectric power dams in Slovenia),* Varstvo narave, Vol. 24, p.p. 85 - 96, 2010 (in Slovene)
[20] IEC 60545: *Guide for Commissioning, Operation and Maintenance of Hydraulic Turbines*, International Electrotechnical Commission, 1976
[21] IEC 62006: *Hydraulic Machines—Acceptance Tests of Small Hydroelectric Installations*, International Electrotechnical Commission, 2010
[22] H.W. Coleman, W.G. Steele: *Experimentation and Uncertainty Analysis for Engineers*, John Wiley and Sons, 1989

Povzetek v slovenskem jeziku

Približne, numerične in eksperimentalne raziskave vodnega udara v hidroelektrarni s cevnimi turbinami Vrhovo. V prispevku raziskujemo učinkovitost in natančnost približnih in numeričnih modelov vodnega udara v slovenskih hidroelektrarnah s cevnimi turbinami na reki Savi. Najprej so predstavljeni približni in numerični modeli togega vodnega udara. Rezultati izračuna so primerjani z rezultati meritev v hidroelektrarni Vrhovo. Izračunane in izmerjene vrednosti so primerjane za obratovalni režim nujne hitre zapore turbine. Vodni udar krmilimo z ustrezno nastavitvijo zakonov zapiranja/odpiranja lopatic vodilnika in gonilnika. Med približnimi in numeričnimi, in izmerjenimi rezultati obstaja dobro ujemanje.